Mathematical analysis of a model for moon-triggered clumping in Saturn's rings

Pedro J. Torres*, Prasanna Madhusudhanan†, Larry W. Esposito†

*Departamento de Matemática Aplicada,
Universidad de Granada, Facultad de Ciencias, Granada, Spain.

†Laboratory of Atmospheric and Space Physics,
University of Colorado, 392 UCB, Boulder, CO 80302, USA.

Email: ptorres@ugr.es, mprasanna@colorado.edu, larry.esposito@lasp.colorado.edu

Abstract

Spacecraft observations of Saturn's rings show evidence of an active aggregation-disaggregation process triggered by periodic influences from the nearby moons. This leads to clumping and break-up of the ring particles at time-scales of the order of a few hours. A mathematical model has been developed to explain these dynamics in the Saturn's F-ring and B-ring [5], the implications of which are in close agreement with the empirical results. In this paper, we conduct a rigorous analysis of the proposed forced dynamical system for a class of continuous, periodic and zero-mean forcing functions that model the ring perturbations caused by the moon flybys. In specific, we derive the existence of at least one periodic solution to the dynamic system with the period equal to the forcing period of the moon. Further, conditions for the uniqueness and stability of the solution and bounds for the amplitudes of the periodic solution are derived.

Keywords: Saturn ring, aggregation-disaggregation process, periodic solution, stability
AMS2000 Subject Classification: 34C25, 85A99.

1 Introduction

In our solar system, all the giant planets have rings. The rings around the planets are flat disks of innumerable small particles that orbit the planet in its equatorial plane [4]. The ring particles range in sizes from dust to boulders to small moonlets. The particles continually collide, resulting in both fragmentation and aggregation. The particles will aggregate into temporary units resembling piles of rubble. Dust and smaller particles collect on the surfaces of larger ones, and can be knocked off to orbit freely, or be re-captured by another particle. The dynamical processes in rings are likely to resemble those in other flattened systems like spiral galaxies, black-hole accretion disks and in the proto-planetary disks where planets form.

The largest and best-studied ring system is Saturn's, which is now being examined at close range by the Cassini space mission. At the time surrounding Saturn's equinox in 2009, when the Sun set on the plane of the rings, Cassini's camera found a surprising number of small objects within the rings by the long shadows that they cast. Thus, the low sun angle provided a unique opportunity to detect larger bodies embedded in Saturn's rings. These observations inspired close analysis of the many star occultations observed by Cassini, when a star's brightness is measured up to a thousand times per second while the star passes behind the rings. This technique yields unprecedented spatial resolution, allowing the detection of objects bigger than a few meters in size. The starlight fluctuations were analyzed by power spectral analysis, indicating clumps 100-2000m in size at the outer edge of Saturn's brightest (B) ring, the same location where the shadow-casting bodies were seen [6]. Small transient clumps are also seen in Saturn's F ring [6, 3]. In both cases,

*P.J. Torres is partially supported by project MTM2011-23652, Spain. P. Madhusudhanan and L. W. Esposito were supported by the NASA Cassini Mission, USA.

the clumps are correlated with the location of nearby moons. This led Esposito to propose [5] that the moon triggers the clumping, particularly at the distances from Saturn where a ring particle's mean orbital motion resonates with that of the moon.

The complicated dynamical interactions in planetary rings are sometimes modeled as a fluid and other times as an example of granular flow [9]. Numerical solutions often rely on N-body simulations (see for instance [7]). Since the ring particle dynamics is so complicated and the N-body solutions are so slow, Esposito et al [5] developed a simplified dynamical model based on some analogies with Plasma Physics. This model solves for the coupled evolution of aggregates and the velocity dispersion at a location within the rings.

The dynamical model proposed in [5] aims to explain the aggregation and disaggregation processes observed in Saturn's F ring and the B ring outer edge due to the perturbation caused by the Saturn's moon, Prometheus and Mimas, respectively. Their numerical simulations demonstrate that the dynamical model explains certain spacecraft measurements corresponding to these regions in the Saturn's ring. Further, these numerical results strongly suggest the existence of a limit cycle for realistic values of the parameters. In this paper, we provide a rigorous mathematical proof of this fact as well as study other features that are relevant from a dynamical point of view.

The model under consideration relates the mean aggregate mass M and the velocity dispersion $v_{\rm rel}^2$ of ring particles at the above mentioned locations in the Saturn's ring, as follows

$$\begin{aligned}\frac{dM}{dt} &= \frac{M}{T_{\rm acc}} - \left(\frac{v_{\rm rel}^2}{v_{\rm th}^2}\right)\frac{M}{T_{\rm coll}}\\ \frac{dv_{\rm rel}^2}{dt} &= -\frac{v_{\rm rel}^2(1-\varepsilon^2)}{T_{\rm coll}} + \frac{M^2}{M_0^2}\frac{v_{\rm esc}^2\left(M_0\right)}{T_{\rm stir}} - f(t).\end{aligned} \tag{1.1}$$

In the first equation of (1.1), the first term refers to the coagulation of the ring particles leading to a growth in the mean aggregate mass at an accretion rate $\frac{1}{T_{\rm acc}}$ ($T_{\rm acc}$ is the accretion period) and the second term refers to the erosion (or break-up) of the larger ring particles due to collisions with other ring particles at collisional rates $\frac{1}{T_{\rm coll}}$($T_{\rm coll}$ is the collisional period) when their velocity dispersion exceed $v_{\rm th}$, the threshold velocity for sticking.

In the second equation of (1.1), the first term refers to the dissipative collisions between the ring particles leading to the reduction in velocity dispersion with ε as the normal coefficient of restitution. The second term refers to the increase in the velocity dispersion to the escape velocity from mass M ($v_{\rm esc}\left(M_0\right)$ is the escape velocity from an aggregate of mass M_0) due to the viscous stirring at a rate $\frac{1}{T_{\rm stir}}$ ($T_{\rm stir}$ is the stirring period), caused by the passage of the ring particles of mass M. Finally, the last term refers to the periodic forcing by the Saturn's moon causing disturbances in the velocity dispersion, where $f(t) = \frac{2\pi v_{th}^2\beta}{T_{\rm syn}}\cos(\frac{2\pi t}{T_{\rm syn}})$ describes the moon perturbation, where $T_{\rm syn}$ is the forcing period, β is the forcing amplitude.

For convenience, we reduce the system to an equivalent dimensionless system with the following substitutions: $x \equiv \frac{M}{M_o}$, $y \equiv \frac{v_{\rm rel}^2}{v_{\rm th}^2}$ and $t \equiv \frac{t}{T_{\rm orb}}$, where $T_{\rm orb}$ is the orbital period of the ring particles around Saturn, and pass to a more mathematical notation by using $\frac{d}{dt} = '$. Then, the system in (1.1) becomes

$$\begin{aligned}x' &= ax - bxy\\ y' &= -cy + dx^2 - f(t)\end{aligned} \tag{1.2}$$

where

$$a = \frac{T_{\rm orb}}{T_{\rm acc}},\ b = \frac{T_{\rm orb}}{T_{\rm coll}},\ c = \frac{T_{\rm orb}(1-\varepsilon^2)}{T_{\rm coll}},\ d = \frac{T_{\rm orb}v_{\rm esc}^2}{T_{\rm stir}v_{\rm th}^2} \tag{1.3}$$

are all positive parameters, $f\left(t\right) = A_o\cos\left(\omega t\right)$, $A_o = \frac{2\pi\beta T_{\rm orb}}{T_{\rm syn}}$, $\omega = \frac{2\pi T_{\rm orb}}{T_{\rm syn}} = \frac{2\pi}{T}$, and T is the (normalized) forcing period.

The above dynamical system has two main differences when compared to the predator-prey system. Firstly, in the second equation, we have the x^2 term instead of the coupling xy. Secondly, the external forcing is not standard in ecological models, since the typical forcing is parametrical (see for instance the model studied in [2]).

Despite these differences, the aggregation-disaggregation model represented by this system can be well explained by drawing an analogy with the predator-prey system. Let the mean aggregate mass of the ring particles correspond to the prey population, and the velocity dispersion correspond to the predator population. The velocity dispersion 'feeds' off the accelerations from the aggregates' gravity (in reference to the second term of the second equation). As the velocity dispersion grows too large, it limits the 'prey' as high velocity collisions lead to to fragmentation of the ring particles (in reference to the second term of the first equation). In the absence of the interaction between the 'predator' and the 'prey', the 'prey' population (mean aggregate mass) grows and the predator population decays (in reference to the first terms of the two equations, respectively). In addition, the predator population is periodically controlled in a certain deterministic manner, as represented by the sinusoidal forcing function.

In the following section, we conduct a thorough qualitative analysis of the above system and comment about the existence and nature of its solution, conditions on uniqueness and asymptotic stability of the solution and finally derive explicit bounds for the solutions. Along with these results, we derive useful insights about the Saturn's ring dynamics based on these results.

Further, the results in this paper hold for any general forcing functions $f(t)$ as long as it is a continuous periodic function of minimal period $T = \frac{2\pi}{\omega}$ with zero mean value, i.e., $\int_0^T f(t)dt = 0$. All the results will be presented for this general forcing function, and the sinusoidal forcing function will be explicitly studied in Section 5.

2 Existence of a periodic solution

Numerical results in [5] strongly suggest the existence of a limit cycle for realistic values of the parameters. In the following theorem, we provide an analytical proof for the same. Further, the result holds for all feasible values of the system parameters.

Theorem 1 *System* (1.2) *has at least one T-periodic solution (x, y) with $x(t) > 0$ for all t.*

Proof. By introducing the change $z = \ln x$, system (1.2) is transformed into

$$\begin{aligned} z' &= a - by \\ y' &= -cy + d\exp(2z) - f(t). \end{aligned} \tag{2.4}$$

The theorem is proved by showing that the above system is equivalent to a second order differential equation of the Duffing type, and then invoking the Landesman-Lazer conditions for the existence of a periodic solution. See Appendix A for the complete proof. □

The above result leads to a physical interpretation that the periodic forcing by the moon gives a limit cycle in the mean aggregate mass and velocity dispersion with the same period as the forcing function.

It is interesting to remark that the latter result can be extended to a family of forcing terms with more complicated recurrence including quasi periodic forcing. The main result in [1] implies the existence of a quasi periodic solution and the boundedness of all solutions in the future.

3 Uniqueness and asymptotic stability

In this section, we derive conditions for the existence of a unique periodic solution and comment about the stability of the solution.

Theorem 2 *When*

$$acT < 2 + \frac{c^2}{2}, \tag{3.5}$$

system (1.2) *has a unique T-periodic solution, which is asymptotically stable.*

Proof. See Appendix B. □

Remark 1 *Observe that for $f \equiv 0$, the unique equilibrium of system* (1.2) *is hyperbolic, hence robust to small perturbations. Therefore, if A_0 is small enough,* (1.2) *presents an asymptotically stable T-periodic orbit. The remarkable feature of the latter result is that stability is proved on a certain region of the involved parameters independently of the size of the external force f.*

As we will see in Section 5, Theorem 2 is applicable to the Saturn's F-ring, in fact for the F-ring $ac = 16\tau^2(1-\varepsilon^2) \simeq 0.104$ so condition (3.5) is satisfied. The condition (3.5) is also satisfied for the Saturn's B-ring outer edge when the optical depth is $\tau = .5$. In the following theorem, a condition for the existence and stability of the solution is derived that depends on the nature of the forcing function via its supremum norm, denoted by $\|f\|_\infty$.

Theorem 3 *Under the assumption*

$$2ac + 2b\|f\|_\infty < \frac{c^2}{4} + \frac{\pi^2}{T^2}, \tag{3.6}$$

system (1.2) *has at least one asymptotically stable T-periodic solution.*

Proof. The above result is obtained by using the technique of lower and upper solutions [8]. See Appendix C for the complete proof. □

In the context of the Saturn's ring dynamics, Theorem 2 and Theorem 3 show that the forced ring system has a limit cycle behavior around the fixed point and when the external forcing satisfies the above condition, it drives a stable limit cycle. Further, the above theorems provide a theoretical justification for the concentric limit cycles that were observed through numerical simulations in [5, Fig. 16 and Fig. 17].

4 Explicit bounds

Theorem 1 provides a general existence result, but more concrete quantitative information about the location of the periodic orbits is desirable. In this section, we derive explicit estimates for the periodic solutions. In the next result, $f^+ = \max\{f, 0\}$, $f^- = \max\{-f, 0\}$ denotes the positive and negative part respectively of a given function f, and $\|f\|_p$ denotes the usual L^p-norm.

Theorem 4 *Let (x, y) with $x(t) > 0$ for all t a T-periodic solution of system* (1.2)*. Then, the following bounds hold*

$$\begin{array}{c} \sqrt{\frac{ac}{bd}}\exp\left(-\frac{\sqrt{T}}{2}\frac{b}{c}\|f\|_2\right) \le x(t) \le \sqrt{\frac{ac}{bd}}\exp\left(\frac{\sqrt{T}}{2}\frac{b}{c}\|f\|_2\right) \\ \frac{a}{b}(1-cT) - \|f^+\|_1 \le y(t) \le \frac{a}{b}(1+cT) + \|f^-\|_1 \end{array} \tag{4.7}$$

for all t.

Proof. The bounds derived above are obtained by working with the second order differential equation of Duffing type (1.12) that is equivalent to the system in (1.2). See Appendix D for the complete proof. □

Since the lower bound for $x(t)$ is non-negative, the T-periodic solution $x(t)$ is also non-negative for all t. The above argument acts as an alternate proof for the later part of the statement in Theorem 1. Further, the bounds derived for the T-periodic solution for $y(t)$ may not necessarily be tight. Especially, for small forcing amplitudes, the T-periodic solutions are expected to be close to the stable feasible fixed point, but the upper and lower bounds deviate from the stable fixed point by a factor of cT about the fixed point. As a result, we derive tighter bounds for $y(t)$ in the following theorem.

Theorem 5 *Alternatively, y satisfies the bounds:*

$$y(t) \ge \max\left(\frac{ab^{-1}cT}{(e^{cT}-1)}, \frac{a\exp\left(-\frac{b\sqrt{T}\|f\|_2}{c}\right)}{b}\right) - \min\left(v_{max}, \sqrt{\frac{\|f\|_2^2(e^{cT}+1)}{2c(e^{cT}-1)}}, \frac{\|f^+\|_\infty}{c}, \frac{\|f^+\|_1}{(1-e^{-cT})}\right) \tag{4.8}$$

$$y(t) \le \min\left(\frac{ab^{-1}cT}{(1-e^{-cT})}, \frac{a\exp\left(\frac{b\sqrt{T}\|f\|_2}{c}\right)}{b}\right) - \max\left(v_{min}, \frac{-\|f^-\|_\infty}{c}, \frac{-\|f^-\|_1}{(1-e^{-cT})}\right), \tag{4.9}$$

where $v_{max} = \max_t \int_{s=t}^{t+T} G(t,s) f(s)\, ds$, $v_{min} = \min_t \int_{s=t}^{t+T} G(t,s) f(s)\, ds$, *and* $G(t,s) = \frac{\exp(cs-ct)}{\exp(cT)-1}$ *is the Green's function.*

Proof. The alternative bounds given by (4.8) and (4.9) are found working directly with the second equation of system (2.4). Given a T-periodic solution $h(t)$, it is known that the unique T-periodic solution of the first-order linear equation $y' + cy = h(t)$ is

$$y = \int_t^{t+T} G(t,s)h(s)ds.$$

Then, from the second equation of system (2.4), we have

$$y = \int_t^{t+T} G(t,s)\left[d\exp(2z) - f(s)\right] ds.$$

Tight upper and lower bounds are derived for each of the two terms in the above integral considered separately. By appropriately combining these bounds, we obtain (4.8) and (4.9). See Appendix E for the complete proof. □

The bounds in (4.8) and (4.9) are tight for small forcing amplitudes. Combining these with the second inequality in (4.7), the bounds are tight for all forcing amplitudes.

Remark 2 *Since y represents a squared relative velocity, a useful lower bound for y should be positive. In this sense, the second bound given by* (4.8) *has the advantage that the lower bound is always positive if the external force f is not too large. In the model case* $f(t) = A_0\cos(\omega t)$, *it is easy to compute* $\|f^+\|_1 = \|f^-\|_1 = 2A_0/\omega$, $\|f\|_2 = A_0\sqrt{\frac{\pi}{\omega}}$, *and the bounds are direct.*

Having completed the mathematical analysis of the system (1.2), in the following section, we consider examples with realistic values of the parameters of the system representing different regions of the Saturn's ring and derive useful insights pertinent to the ring dynamics.

5 Insights on Saturn's ring dynamics

We begin with some corollaries of the theorems presented in the previous sections for the Saturn's ring system.

Remark 3 *The non-trivial, feasible stable fixed point for the unforced dynamic system is* $\left(M, v_{\text{rel}}^2\right) = \left(\sqrt{\frac{T_{\text{stir}}(1-\varepsilon^2)}{v_{\text{esc}}^2(M_o)T_{\text{acc}}}},\ \frac{T_{\text{coll}}}{T_{\text{acc}}}\right)$. *When externally forced by periodic perturbations from the Saturn's moons, the mean aggregate mass and the velocity dispersion demonstrates periodic aggregation-disaggregation cycle with the same period as that of the moon's forcing.*

Corollary 1 *(of Theorem 2) There exists a unique, asymptotically stable limit-cycle for the* (M, v_{rel}^2) *system if the forcing period satisfies the condition*

$$T < \frac{1 + 4\tau^2\left(1-\varepsilon^2\right)^2}{8\tau^2\left(1-\varepsilon^2\right)}, \tag{5.10}$$

where the right-hand-side depends on the mean optical depth and the normal coefficient of restitution corresponding to the specific location in the Saturn's ring system.

The realistic parameters corresponding to the Saturn's ring system are $\varepsilon = 0.6$, $T_{\text{syn}} = T_{\text{orb}} = T = 1$. The optical depth is $\tau = 0.1$ for the F-ring and $\tau = 1.5,\ 1,\ 0.5$ for the B-ring outer edge. Hence, our result is applicable to the F-ring and also to the B-ring outer edge when $\tau = 0.5$.

Now, we consider a systematic study of each region in the Saturn's rings, and start with the dynamics of the B-ring outer edge.

Corollary 2 *For a sinusoidal forcing function, $f(t) = \frac{2\pi\beta}{T}\cos\left(\frac{2\pi t}{T}\right)$, the upper and lower bounds of the T-periodic solution for the mass of the aggregate is*

$$\mathrm{e}^{\frac{-\pi\beta}{\sqrt{2}(1-\varepsilon^2)}} \leq \frac{M(t)}{2\sqrt{4\tau T_{\mathrm{stir}}(1-\varepsilon^2)}} \leq \mathrm{e}^{\frac{\pi\beta}{\sqrt{2}(1-\varepsilon^2)}}. \tag{5.11}$$

For $v_{\mathrm{rel}}^2(t)$, the bounds are obtained from Theorems 4 and 5 with $a = b = \frac{c}{1-\varepsilon^2} = 4\tau$, $v_{\mathrm{esc}}(M_0) = 0.5m/sec$, $v_{\mathrm{th}} = 1m/sec$, $v_{max} = -v_{min} = \frac{2\pi\beta}{c\sqrt{c^2T^2+4\pi^2}}$, $\|f\|_2 = \sqrt{\int_{t=0}^{T}|f(t)|^2\,dt} = \pi\beta\sqrt{\frac{2}{T}}$, $\|f^+\|_1 = \int_{t=0}^{T}|f^+(t)|\,dt = 2\beta$, , $\|f^+\|_1 = \int_{t=0}^{T}|f^-(t)|\,dt = 2\beta$, and $\|f\|_\infty = \frac{2\pi\beta}{T}$.

We begin with studying the impact of varying the stirring rate $f_{\mathrm{stir}} = \frac{1}{T_{\mathrm{stir}}}$ on the amplitudes of the periodic solutions of $\left(M(t), v_{\mathrm{rel}}^2(t)\right)$, and Figures 1a - 1c plot the maxima and minima of the T-periodic solution of the $\left(M, v_{\mathrm{rel}}^2\right)$ system obtained using numerical simulations against the derived upper and lower bounds for the T-periodic solution of the $\left(M, v_{\mathrm{rel}}^2\right)$ system from Theorem 4 and Theorem 5. The system parameters corresponding to the Saturn's ring system are $\varepsilon = 0.6$, $T_{\mathrm{syn}} = T_{\mathrm{orb}}$ $(T = 1)$, $\beta = 0.5$ and $\tau = 1.5,\ 1$, and 0.5 for Figure 1a, Figure 1b and Figure 1c, respectively. The Saturn's B-ring including the Janus 2:1 density wave, and the B-ring outer edge have 1.5 and 1 as the typical values for the optical depth. Further, $\tau = 0.5$ is the typical optical depth value for the Saturn's A ring, Mimas 5:3 density wave and the Janus 6:5 density wave.

From (5.11), it is clear that the amplitude upper and lower bounds for the periodic solutions of $M(t)$ vary log-linearly with f_{stir}, and hence the corresponding curves in the plot are straight lines. It is interesting to note that the actual values for the maximum and minimum amplitudes (obtained through simulations) also appear to have a log-linear relationship with f_{stir} with the same slope as that of the upper and lower bounds. As a result, an exponential increase in f_{stir} causes an exponential decay in the mean aggregate mass of the ring particles. This effect can be understood as follows. Large f_{stir} causes the rate of change of $y(t)$ to be positive, and once $v_{\mathrm{rel}}^2(t) > \frac{T_{coll}}{T_{acc}}$ (same as $y > \frac{a}{b}$ in (2.4)), this causes a negative slope for $M(t)$, and essentially causing the exponential decay of $M(t)$. Further, the parameter f_{stir} has a negligible effect on the amplitudes of $v_{\mathrm{rel}}^2(t)$, as is evident from the negligible slope in the figure above. Notice that both the axes are in log-scale and the plots for the lower-bound of $v_{\mathrm{rel}}^2(t)$ does not appear in the plot because it takes negative values for all values of f_{stir}.

We see that the effect of changing τ only changes the magnitudes of maxima, minima, and the bounds on $M(t)$ and $v_{\mathrm{rel}}^2(t)$. Otherwise, $M(t)$ has a log-linear relationship with f_{stir}, with the same slope for all values of τ. Comparing Figures 1a - 1c, the magnitudes of maxima $M(t)$ increases with increase in τ, and the minima decreases with increase in τ. Further, the magnitude of the maxima of $v_{\mathrm{rel}}^2(t)$ remains unchanged with increase in τ and the magnitude of the minima decreases with increase in τ. The physical interpretation is that larger optical depth leads to a larger mean aggregate mass, but not large velocity dispersion. This is because the velocity dispersion is pegged near the fixed point value given by the strong erosion for $v_{\mathrm{rel}}^2(t) > v_{\mathrm{th}}^2$, which reverses the growth of $M(t)$. For the same reason, increasing f_{stir} reduces the upper value for $M(t)$.

Next, we study the impact of varying the forcing amplitude β on the periodic solutions of $\left(M(t), v_{\mathrm{rel}}^2(t)\right)$, and Figures 2a - 2c plot the maxima and minima of the T-periodic solution of the $\left(M, v_{\mathrm{rel}}^2\right)$ system obtained using numerical simulations against the derived upper and lower bounds for the T-periodic solution of the $\left(M, v_{\mathrm{rel}}^2\right)$ system from Theorem 4 and Theorem 5. The system parameters are the same as before and the stirring period is assumed to be equal to the orbital period of the ring particles around Saturn, in other words, $f_{\mathrm{stir}} = 1$.

Notice that for small forcing amplitudes, the periodic solutions for $M(t)$ and $v_{\mathrm{rel}}^2(t)$ has a small amplitude about their average values, which in this case, are the asymptotically stable fixed points (see Remark 3) of the corresponding autonomous system of differential equations. With increase in β, we see an increasing deviations in the amplitude of $M(t)$ about the average values, while still non-negative, since the lower-bound from (5.11) is non-negative. Translating to the physical phenomena, the ring particle aggregates tend to achieve large masses as well as negligibly small masses, with increase in the forcing amplitude, in each period.

The increase in forcing amplitudes causes a similar effect on $v_{\mathrm{rel}}^2(t)$ as on $M(t)$. But increasing the forcing amplitude beyond a certain threshold causes $v_{\mathrm{rel}}^2(t)$ to take negative values, which is non-physical.

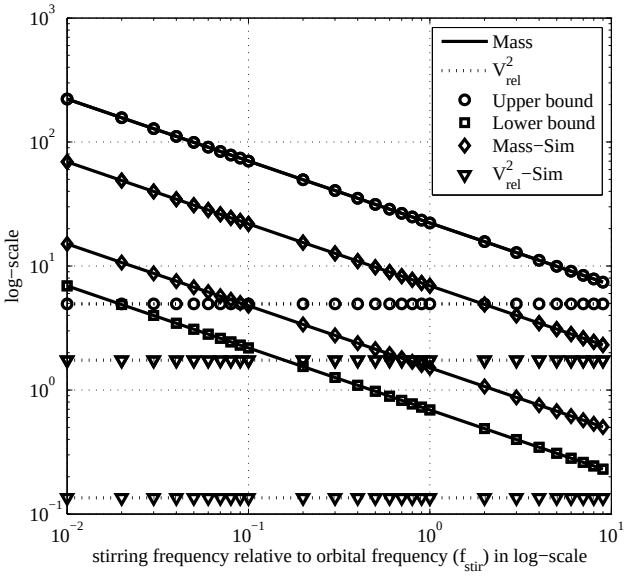

(a)

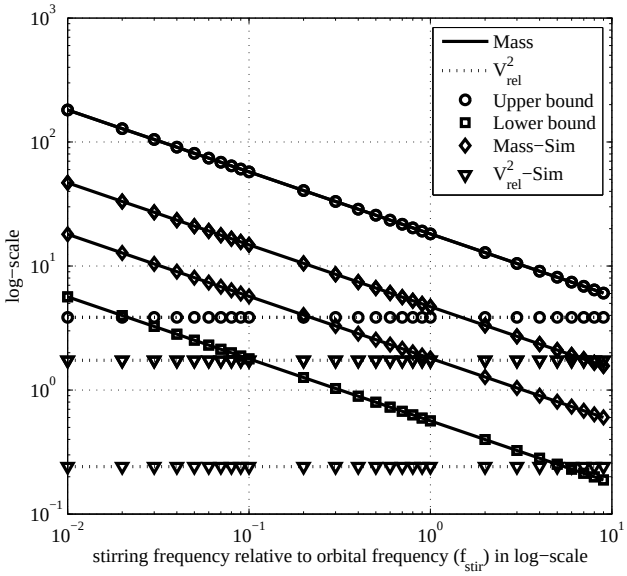

(b)

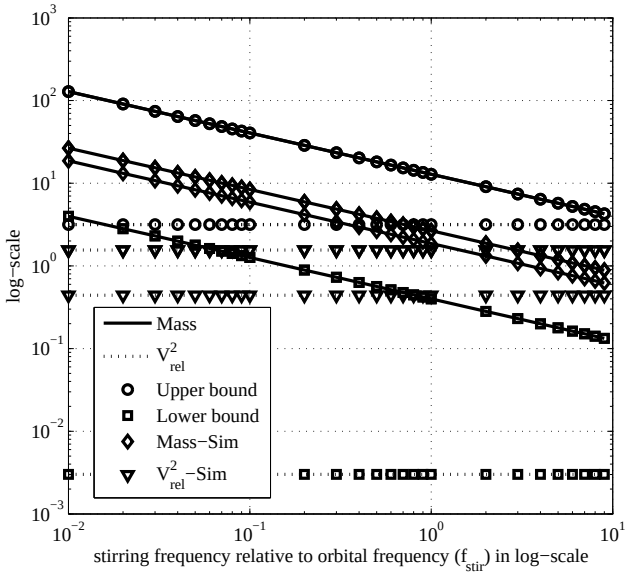

(c)

Figure 1: **Derived bounds compared to numerical simulations for varying $f_{\rm stir}$:** The system parameters corresponds to the B-ring outer edge where the normal coefficient of restitution $\varepsilon = 0.6$, the forcing period of the moon is equal to the orbital period of the ring particles about Saturn ($T = 1$) and the forcing amplitude $\beta = 0.5$. (a) The mean optical depth is $\tau = 1.5$, (b) the mean optical depth is $\tau = 1$ and (c) the mean optical depth is $\tau = 0.5$.

This sets a strict upper limit on the forcing amplitude, which in the case of the above figure, happens around $\beta = 0.6$. Comparing Figure 2a and 2c, as τ increases from 0.5 to 1.5, $M(t)$ maxima increases, $v_{\text{rel}}^2(t)$ maxima changes only slightly.

Finally, notice that the upper and lower bounds for $M(t)$ and $v_{\text{rel}}^2(t)$ are tight for small forcing amplitudes. This means that the behavior of the system is well-characterized by the bound derived in Theorem 4 and Theorem 5 for the regions in the Saturn's ring system where the influence of the moons are negligible. The analytical results provide a reasonable idea about the nature of the system and parallel the explicit numerical simulations.

6 Conclusions

We consider the mathematical model developed in [5] for understanding the dynamics of certain specific locations in the Saturn's ring system due to the periodic perturbations caused by the nearby moon. This model relates the mean aggregate mass and the velocity dispersion of the ring particles at a certain location in the Saturn's ring system in a manner similar to the popular predator-prey model in ecology, although it represents a totally different physical phenomenon. Further, this has been studied purely using numerical simulations so far.

In this paper, we conduct a rigorous mathematical analysis of the dynamical system and derive results pertaining to the existence, uniqueness and stability of its solution. We analytically prove that the dynamical system causes a periodic solution for the mean aggregate mass and the velocity dispersion of the ring particles at a period equal to the forcing period of the moon. Further, upper and lower bounds for the solution to the system are derived, that are especially tight for small perturbations caused by the moons. These bounds well-characterize the dependence of the system solution on various system parameters. Several useful insights are drawn about the Saturn's ring system based on the theoretical results presented here.

References

[1] S. Ahmad, A Nonstandard Resonance Problem for Ordinary Differential Equations, Transactions of the American Mathematical Society, Vol. 323, No. 2 (Feb., 1991), pp.857-875.

[2] Z. Amine, R. Ortega, A periodic prey-predator system, J. Math. Anal.Appl. 185 (1994), 477-489.

[3] K. Beurle, C.D. Murray, G.A. Williams, M.W. Evans, N.J. Cooper, C.B. Agnor, Direct evidence for gravitational instability and moonlet formation in Saturn's rings, Astophys. J. 718 (2010), 176-180

[4] L.W. Esposito, Planetary Rings, Cambridge University Press (2006).

[5] L.W. Esposito, N. Albers, B.K. Meinke, M. Sremčević, P. Madhusudhanan, J.E. Colwell, R.G. Jerousek, A predator-prey model for moon-triggered clumping in Saturn's rings, Icarus 217 (2012), 103-114.

[6] L.W. Esposito, B. K. Meinke, J.E. Colwell, P.D. Nicholson, M.M. Hedman, Moonlets and Clumps in Saturn's F Ring, Icarus Vol 194/1 (2008), 278-289.

[7] M.C. Lewis, G.R. Stewart, Features around embedded moonlets in Saturn's rings: The role of self-gravity and particle size distributions, Icarus 199 (2009), 387-412.

[8] F.I. Njoku and P. Omari, Stability properties of periodic solutions of a Duffing equation in the presence of lower and upper solutions, Appl. Math. Comput. 135 (2003), 471-490.

[9] J. Schmidt, K. Ohtsuki, N. Rappaport, H. Salo, F. Spahn, Dynamics of Saturn's Dense Rings, in *Saturn from Cassini-Huygens*, by M.K. Dougherty, L.W. Esposito, S.M. Krimigis, ISBN 978-1-4020-9216-9. Springer Science+Business Media B.V., 2009, p. 413.

[10] G. Talenti, Best constant in Sobolev inequality, Ann. Mat. Pura Appl. 4 (1976) 353-372.

[11] P.J. Torres, Existence and stability of periodic solutions of a Duffing equation by using a new maximum principle, Mediterranean Journal of Mathematics 1, n.4 (2004), 479-486.

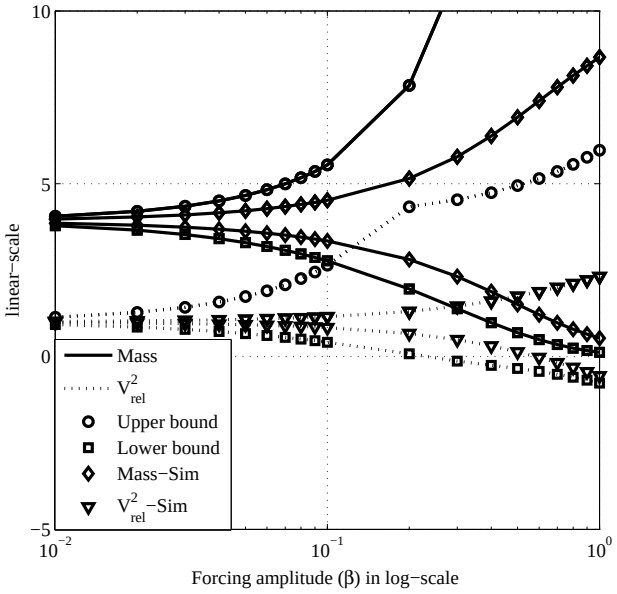

(a)

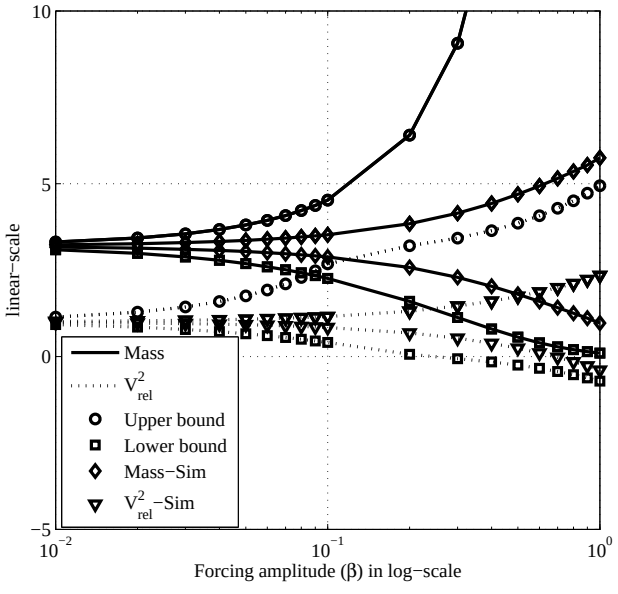

(b)

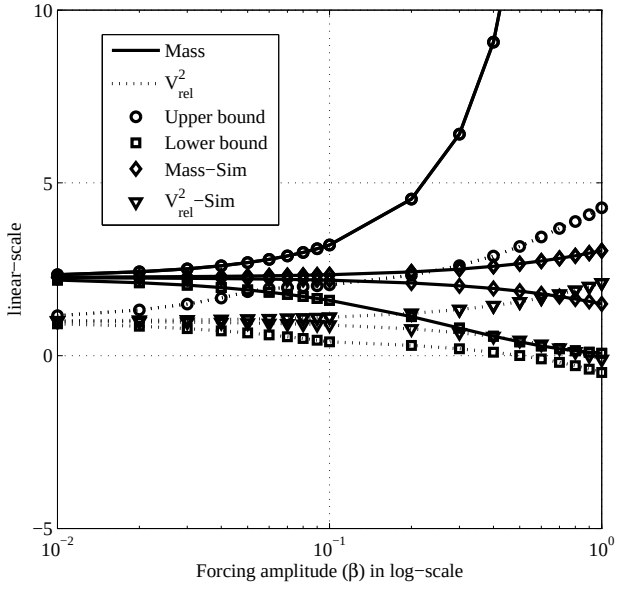

(c)

Figure 2: **Derived bounds compared to numerical simulations for varying forcing amplitude β:** The system parameters corresponds to the B-ring outer edge where the normal coefficient of restitution $\varepsilon = 0.6$, the forcing period of the moon and the stirring period are both equal to the orbital period of the ring particles about Saturn ($T = f_{\text{stir}} = 1$). (a) The mean optical depth is $\tau = 1.5$, (b) the mean optical depth is $\tau = 1$ and (c) the mean optical depth is $\tau = 0.5$.

[12] J.R. Ward, Periodic solutions for a class of differential equations, Proc. Amer.Math.Soc. 78 (1980), 350-352.

A Proof for Theorem 1

Deriving the first equation and inserting the second one, we obtain the following second order differential equation of Duffing type

$$z'' + cz' + bd\exp(2z) = ac + bf(t). \tag{1.12}$$

Now the periodic problems for (1.2) and (1.12) are completely equivalent. If (x, y) is a T-periodic solution of system (1.2) with $x(t) > 0$ for all t, then $z = \ln x$ is a T-periodic solution of (1.12). Conversely, if z is a T-periodic solution of eq. (1.12), then $x = \exp(z), y = (a - z')/b$ is a T-periodic solution of system (1.2) with $x(t) > 0$ for all t.

Since $ac > 0$, eq. (1.12) is of Landesman-Lazer type. Landesman-Lazer conditions are classical and implies the existence of a periodic solution, see for instance [12, Theorem 1].

B Proof for Theorem 2

We know that system (1.2) is equivalent to eq. (1.12), hence along this proof we will work directly with this last equation.

Uniqueness. Assume that z_1, z_2 are two T-periodic solutions of eq. (1.12). The difference $\delta(t) = z_1(t) - z_2(t)$ is a solution of a second order linear equation

$$\delta'' + c\delta' + h(t)\delta = 0, \tag{2.13}$$

where $h(t) = bd\frac{\exp(2z_1)-\exp(2z_2)}{z_1-z_2}$. We consider two cases:

- *Case 1*: $\delta(t) \neq 0$ for every t: without loss of generality, we may take $\delta(t) > 0$. By the Mean Value Theorem,
$$h(t) = 2bd\exp(2\xi(t)),$$
where $z_2(t) < \xi(t) < z_1(t)$ for every t. Hence, by using (4.15), one obtains
$$\|h\|_1 = 2bd\int_0^T \exp(2\xi(t))dt < 2bd\int_0^T \exp(2z_1(t))dt = 2acT.$$
Using (3.5), one may check easily that $h \in \Omega_{1,c}$, as defined in [11, Section 3]. Then, by [11, Corolllary 2.5], the operator defined by the left-hand side of (2.13) is inversely positive, in particular (2.13) is non-degenerate and its only periodic solution is the trivial one, which is a contradiction with the assumption that $\delta(t) \neq 0$ for every t.

- *Case 2*: $\delta(t_0) = 0$ for some $t_0 \in [0, T]$: by periodicity, there exists $t_1 > t_0$ such that $d(t_1) = 0$ and $\delta(t) \neq 0$ for all $t \in]t_0, t_1[$. Again, we may assume without losing generality that $\delta(t) > 0$ for all $t \in]t_0, t_1[$. Define the truncated function $\hat{h}(t)$ as $h(t)$ if $t \in [t_0, t_1]$ and 0 if $t \in [0, t_0[\cup]t_1, T]$. By reasoning as before, $h \in \Omega_{1,c}$. Then, as a consequence of the results in [11] (see Remark 2.2 therein), the distance between two consecutive zeroes of a solution of $\delta'' + c\delta' + \hat{h}(t)\delta = 0$ is greater than T, but δ is a solution vanishing at t_0, t_1, which is a contradiction.

After this analysis, the only remaining possibility is $d(t) = 0$ for every t, so the T-periodic solution is unique.

Stability. The proof for asymptotic stability is also based on the results from [11]. Let $z(t)$ be the unique T-periodic solution of eq. (1.12). A standard computation gives that the topological index of z is $\gamma(z) = 1$. The variational equation is $u'' + cu' + h(t)u = 0$ with $h(t) = 2bd\exp(2z(t))$ and again $h \in \Omega_{1,c}$ as a result of (3.5). Then the asymptotic stability follows directly from [11, Theorem 3.1].

C Proof for Theorem 3

We use the terminology and notation from [8]. A lower solution is found by fixing a constant α such that

$$bd\exp(2\alpha) = ac + b\left\|f\right\|_\infty. \tag{3.14}$$

An upper solution is easily obtained as follows. Take F the unique T-periodic solution of $z'' + cz' = f(t)$ with mean value zero. Then, $\beta(t) = -M + F(t)$ with M big enough is an upper solution with $\beta < \alpha$. To apply [8, Theorem 1.2], we have to check two hypotheses. The fist one is the finiteness of the number of T-periodic solutions, which is direct from the analiticity of the field on the state variables. The second hypothesis is condition (1.6) in [8]. Fix $g(t,z) = bd\exp(2z) - ac - bf(t)$. For $s \in [\beta(t), \alpha]$,

$$\frac{\partial}{\partial s}g(t,s) = 2bd\exp(2s) \leq 2bd\exp(2\alpha) = 2ac + 2b\left\|f\right\|_\infty < \frac{c^2}{4} + \frac{\pi^2}{T^2}$$

by (3.6), which is just (1.6) in [8]. The result is done.

D Proof for Theorem 4

We work again over the equivalent eq. (1.12). Integrating (1.12) over a whole period

$$bd\int_0^T \exp(2z)dt = acT. \tag{4.15}$$

By the integral mean value theorem, there exists $t_0 \in [0,T]$ such that

$$\exp(2z(t_0)) = \frac{ac}{bd}. \tag{4.16}$$

Observe that $z(t) - z(t_0) \in H_0^1(t_0, T+t_0)$, then by the Sobolev inequality with the optimal constant (see for instance [10]), we get

$$|z(t) - z(t_0)| \leq \frac{\sqrt{T}}{2}\left\|z'\right\|_2. \tag{4.17}$$

On the other hand, multiplying (1.12) by z' and integrating over $[0,T]$ and applying Cauchy-Schwarz inequality, we get

$$c\left\|z'\right\|_2^2 = b\int_0^T f(t)z'dt \leq b\left\|f\right\|_2\left\|z'\right\|_2,$$

hence,

$$\left\|z'\right\|_2 \leq \frac{b}{c}\left\|f\right\|_2. \tag{4.18}$$

Now, combining (4.16),(4.17) and (4.18),

$$z(t) = z(t_0) + z(t) - z(t_0) \leq \frac{1}{2}\ln\left(\frac{ac}{bd}\right) + \frac{\sqrt{T}}{2}\frac{b}{c}\left\|f\right\|_2$$

and

$$z(t) = z(t_0) + z(t) - z(t_0) \geq \frac{1}{2}\ln\left(\frac{ac}{bd}\right) - \frac{\sqrt{T}}{2}\frac{b}{c}\left\|f\right\|_2.$$

The first inequality of (4.7) arises from here taking $z = \ln x$ and finding the value of x.

The bound for y is found as follows. Let t_* such that $z(t_*) = \min_{t\in[0,T]} z(t)$. Integrating (1.12) on $[t_*, t]$,

$$z'(t) + cz(t) - cz(t_*) + bd\int_{t_*}^t \exp(2z)dt = \int_{t_*}^t ac + bf(s)ds \leq acT + b\left\|f^+\right\|_1.$$

Since $cz(t) - cz(t_*) + bd\int_{t_*}^{t} \exp(z)dt \geq 0$, then

$$z'(t) \leq \int_{t_*}^{t} ac + bf(s)ds \leq acT + b\left\|f^+\right\|_1. \tag{4.19}$$

Analogously, Let t^* such that $z(t^*) = \max_{t\in[0,T]} z(t)$. Integrating (1.12) on $[t^*, t]$,

$$z'(t) + cz(t) - cz(t^*) + bd\int_{t^*}^{t} \exp(2z)dt = \int_{t^*}^{t} ac + bf(s)ds \geq -b\left\|f^-\right\|_1.$$

Then,

$$z'(t) \geq -bd\int_{t^*}^{t} \exp(z)dt - b\left\|f^-\right\|_1 \geq -bd\int_{t^*}^{t^*+T} \exp(z)dt - b\left\|f^-\right\|_1.$$

Since $z(t)$ is T-periodic, $\int_{t^*}^{t^*+T} \exp(2z)dt = \int_0^T \exp(2z)dt$, then by using (4.15),

$$z'(t) \geq -acT - b\left\|f^-\right\|_1. \tag{4.20}$$

Finally, inserting (4.19) − (4.20) into $y = \frac{1}{b}(a - z')$, one obtains the second inequality of (4.7).

E Proof for Theorem 5

Note that

$$\frac{1}{\exp(cT) - 1} \leq G(t,s) \leq \frac{\exp(cT)}{\exp(cT) - 1}$$

for all $t, s \in [0, T]$.

In the following steps, we derive upper and lower bounds for both the terms in the above expression, which will be used later to obtain bounds for $y(t)$.

Bounds for $u(t) = \int_{s=t}^{t+T} G(t,s)\exp(2z(s))\,ds$:

Using the bounds for $G(t,s)$,

$$\frac{acT}{bd\left(\mathrm{e}^{cT} - 1\right)} \leq u(t) \leq \frac{acT\mathrm{e}^{cT}}{bd\left(\mathrm{e}^{cT} - 1\right)}. \tag{5.21}$$

The next set of bounds are derived by using the bounds derived for $z(t)$ in the proof of Theorem 4 and noting that $\int_{s=t}^{t+T} G(t,s)\,ds = \frac{1}{c}$

$$\frac{a}{bd}\exp\left(-\frac{b\sqrt{T}\left\|f\right\|_2}{c}\right) \leq u(t) \leq \frac{a}{bd}\exp\left(\frac{b\sqrt{T}\left\|f\right\|_2}{c}\right). \tag{5.22}$$

Combining (5.21) and (5.22) , we get

$$\max\left(\frac{acT}{bd\left(\mathrm{e}^{cT} - 1\right)}, \frac{a}{bd}\exp\left(-\frac{b\sqrt{T}\left\|f\right\|_2}{c}\right)\right) \leq u(t) \leq \min\left(\frac{acT\mathrm{e}^{cT}}{bd\left(\mathrm{e}^{cT} - 1\right)}, \frac{a}{bd}\exp\left(\frac{b\sqrt{T}\left\|f\right\|_2}{c}\right)\right). \tag{5.23}$$

Bounds for $v(t) = \int_{s=t}^{t+T} G(t,s)f(s)\,ds$:

Let $p(t,s) \triangleq \frac{G(t,s)}{\int_{s=t}^{t+T} G(t,s)ds}$. We know, $\int_{s=t}^{t+T} G(t,s)\,ds = \frac{1}{c}$. Hence, $v(t) = \frac{1}{c}\int_{s=t}^{t+T} p(t,s)f(s)\,ds$. Since $f_{min} \leq \int_{s=t}^{t+T} p(t,s)f(s)\,ds \leq f_{max}$, we have the first set of bounds

$$\frac{f_{min}}{c} \leq v(t) \leq \frac{f_{max}}{c}. \tag{5.24}$$

Similarly, using the Cauchy-Schwartz inequality, we have $\int_{s=t}^{t+T} p(t,s) f(s)\, ds \leq \|f\|_2 \sqrt{\int_{s=t}^{t+T} p^2(t,s)\, ds}$ and hence

$$v(t) \leq \|f\|_2 \sqrt{\frac{e^{cT}+1}{2c(e^{cT}-1)}}. \tag{5.25}$$

Another set of bounds based on the following inequality

$$-\int_{s=t}^{t+T} G(t,s) f^-(s)\, ds \leq v(t) \leq \int_{s=t}^{t+T} G(t,s) f^+(s)\, ds$$

are

$$\frac{-\|f^-\|_\infty}{c} \leq v(t) \leq \frac{\|f^+\|_\infty}{c} \tag{5.26}$$

$$\frac{-\|f^-\|_1 e^{cT}}{(e^{cT}-1)} \leq v(t) \leq \frac{\|f^+\|_1 e^{cT}}{(e^{cT}-1)}. \tag{5.27}$$

And finally, if the $v(t)$ is computable for all t, then,

$$v_{min} \leq v(t) \leq v_{max}. \tag{5.28}$$

Note that (5.24) and (5.26) are equivalent. Hence, combining (5.25) - (5.28), we get

$$\begin{aligned} v(t) &\geq \min\left(v_{min}, \frac{-\|f^-\|_\infty}{c}, \frac{-\|f^-\|_1 e^{cT}}{(e^{cT}-1)}\right) \\ v(t) &\leq \min\left(v_{max}, \|f\|_2 \sqrt{\frac{e^{cT}+1}{2c(e^{cT}-1)}}, \frac{\|f^+\|_\infty}{c}, \frac{\|f^+\|_1 e^{cT}}{(e^{cT}-1)}\right). \end{aligned} \tag{5.29}$$

Using (5.23) and (5.29), (4.8) and (4.9) follow directly.